

# Photoinduced Decomposition of Trichloroethylene on Soil Components

TING TAO, JANE J. YANG, AND  
GARY E. MACIEL\*

Department of Chemistry, Colorado State University,  
Fort Collins, Colorado 80523

The photoinduced decomposition of trichloroethylene adsorbed on Ca-montmorillonite by long-wavelength UV irradiation has been studied in a quartz tube open to air or through which air or oxygen is passed. Solid-sample and liquid-solution NMR techniques were used to identify apparent products or intermediates of the photodecomposition. Dichloroacetic acid was identified as a major organic product/intermediate; substantial amounts of pentachloroethane and trichloroacetic acid were also identified. The formation of CO<sub>2</sub> was characterized quantitatively by wet chemical analysis. About 40% and 57%, respectively, of the total carbon of trichloroethylene was converted to carbon dioxide in air and O<sub>2</sub> environments over a period of 16 days. Phosgene and HCl were also detected. The photodecomposition of trichloroethylene adsorbed on whole soil, on Zn<sup>2+</sup>-exchanged and Cu<sup>2+</sup>-exchanged montmorillonites, on kaolinite, and on silica gel was also examined in less detail; qualitatively, the conversion of trichloroethylene to dichloroacetic acid in a 48-h period occurred with the following order of decreasing efficiencies: Zn<sup>2+</sup>-montmorillonite > silica gel > kaolinite > Ca<sup>2+</sup>-montmorillonite > whole soil > Cu<sup>2+</sup>-montmorillonite. These results show that the photoinduced decomposition of adsorbed trichloroethylene occurs on a variety of adsorbents, generating products and intermediates that are similar to what have been reported previously for TiO<sub>2</sub>-based photodecomposition but with much longer time scales. These conversions can, therefore, be expected to occur in sunlight at the air–soil interface.

## Introduction

Trichloroethylene (TCE), an Environmental Protection Agency (EPA) priority pollutant (1), has been used in a wide range of industrial processes, e.g., for degreasing metals and for dry cleaning (2). As a result of its leaking from underground storage tanks and improper disposal practices, TCE has been identified in at least half of the sites of the National Priorities List (Superfund sites) (3, 4) and represents one of the most frequently detected contaminants of national concern in hazardous waste sites (5). Consequently, it is important to know the chemical behavior and fate of TCE in the environment. One aspect of this complex issue is photochemical behavior of TCE at the air–soil interface.

In addition to the development of bioremediation techniques aimed at degrading TCE in groundwater (6, 7),

extensive research has been reported on the photoassisted decomposition of TCE on TiO<sub>2</sub>(s) photocatalysts as an alternative environmental remediation method to destroy TCE efficiently (8–17). In the reported studies, the photocatalytic oxidation of TCE in low concentration (ppm level) was investigated at TiO<sub>2</sub>(s) interfaces with the gas phase (including air or oxygen), or with an aqueous solution, by such instrumental methods as IR (11–13, 16), GC (16, 17), and MS (13, 14, 16). The “total mineralization” of TCE to CO<sub>2</sub> and HCl has been reported for some conditions (18, 19). Intermediate products have also been observed during the photodegradation of TCE on TiO<sub>2</sub>(s) catalysts; among them are dichloroacetic acid, dichloroacetyl chloride, dichloroacetylaldehyde, trichloroacetic acid, trichloroacetylaldehyde, phosgene, and other products (11–17). Various mechanisms have been proposed for TCE photooxidation on a TiO<sub>2</sub>(s) surface. Some researchers have suggested that hydroxyl radicals or hydroperoxide radicals initiate the decomposition of TCE (12, 19). Other researchers have suggested that TCE is oxidized in chain reactions initiated by chlorine atoms (13, 14, 20) or that TCE is oxidized on TiO<sub>2</sub>(s) by electronically activated O<sub>2</sub> (11). Recently, Raftery and co-workers (21,22) reported an in situ solid-state <sup>13</sup>C NMR (nuclear magnetic resonance) study of the degradation of <sup>13</sup>C-labeled TCE, in which they characterized the reactions of TCE over TiO<sub>2</sub>(s) photocatalysts and identified reaction intermediates and products in the complex surface chemistry.

High-resolution solid-state NMR techniques (23) have begun to emerge among the host of investigative methods used in elucidating the interactions of organic pollutants with soil or its major components (24–26). The orientation of the study reported here is not the search for improved remediation methodology but rather to find out what photoactivated processes might occur with TCE at the air–soil interface due to sunlight. The major focus of the work presented here was to study the chemical behavior of trichloroethylene on Ca-montmorillonite and, to lesser extents, whole soil and other adsorbents, induced by irradiation by long-wavelength UV light under conditions similar to what might be experienced by TCE due to sunlight at the air–soil interface. Because the TCE that was used in this study contains <sup>13</sup>C in only its natural abundance (1.1%) and because of the relatively low inherent sensitivity of NMR, this study employed much larger loading levels than one expects in naturally occurring samples in the environment.

One can expect that many, if not most, of the chemical transformations observed in this study will also occur at much lower (e.g., environmentally “relevant”) TCE concentrations, especially since similar product/intermediate species have been reported from previous studies based on other techniques and much lower TCE loading levels; however, the results of this paper cannot be extrapolated *quantitatively* to lower TCE levels until the relevant kinetic orders are determined. We believe that the results reported here can provide useful information on important aspects of the *qualitative* chemical behavior of a contaminated site. This study shows that the same kind of photoinduced products that have been reported previously from TiO<sub>2</sub>-based photodecompositions can also be generated photochemically from trichloroethylene adsorbed on soil components present at the soil–air interface, albeit on a slower time scale.

## Experimental Section

**Materials.** Trichloroethylene (ACS reagent grade) was purchased from Fisher Chemical Company and used as received without further purification. Ca-montmorillonite

\* Corresponding author phone: (970)491-6480; fax: (970)491-1801; e-mail: maciel@lamar.colostate.edu.

(STx-1) and kaolinite (KGa-1b) were purchased from the Clay Minerals Repository of the University of Missouri at Columbia and used as received. The chemical composition (wt %) of the Ca-montmorillonite is SiO<sub>2</sub>, 70.1; Al<sub>2</sub>O<sub>3</sub>, 16.0; TiO<sub>2</sub>, 0.22; Fe<sub>2</sub>O<sub>3</sub>, 0.65; FeO, 0.15; MnO, 0.009; MgO, 3.69; CaO, 1.59; Na<sub>2</sub>O, 0.27; K<sub>2</sub>O, 0.078; P<sub>2</sub>O<sub>5</sub>, 0.026; S, 0.04; and F, 0.084. The chemical composition of the kaolinite is SiO<sub>2</sub>, 44.2; Al<sub>2</sub>O<sub>3</sub>, 39.7; TiO<sub>2</sub>, 1.39; Fe<sub>2</sub>O<sub>3</sub>, 0.13; FeO, 0.08; MnO, 0.002; MgO, 0.03; Na<sub>2</sub>O, 0.013; K<sub>2</sub>O, 0.050; P<sub>2</sub>O<sub>5</sub>, 0.034; and F, 0.013. The water contents of the Ca-montmorillonite (STx-1) and kaolinite (KGa-1b) employed were 15% and 10%, respectively, determined by weight loss upon dehydration at 150 °C under vacuum (10<sup>-3</sup> Torr). The Clay Minerals Repository provided the following information on the clays: The Ca-montmorillonite has a surface area of 83.8 m<sup>2</sup>/g with 200–300 mesh particle size, and the kaolinite has a surface area of 10.1 m<sup>2</sup>/g with 200–300 mesh particle size. The interlayer space is 15.17 Å for Ca-montmorillonite and 7.11 Å for kaolinite, based on packed powder XRD results. The carbon contents are less than 0.3% (~0.2% CO<sub>2</sub>) in both the Ca-montmorillonite and kaolinite. Zn<sup>2+</sup>-exchanged and Cu<sup>2+</sup>-exchanged Ca-montmorillonites were prepared by stirring 500 mL of 1.0 M ZnCl<sub>2</sub>(aq) and 1.0 M CuCl<sub>2</sub>(aq) solutions, respectively, with 40.0 g Ca-montmorillonite (as received) at 25 °C for 1 day. In each experiment, the resulting suspension was divided into six portions; each portion was washed with 250 mL of water and then centrifuged. The solids were dried at 25 °C under vacuum (10<sup>-3</sup> Torr). The compressed air and O<sub>2</sub>(g) were obtained from General Air Company. Silica gel (S679–500) was obtained from Fisher Chemical Company and used as received. The soil sample was collected from the Uncompahgre National Forest of southwestern Colorado, about 4 in. below the "leaf litter". A detailed characterization of this soil will be published elsewhere (27).

**UV Source.** The UV source is a 100-W long-wavelength UV lamp (Model B-100Ap from UVP Inc, Upland, CA). The intensity maximum of this UV lamp occurs at a wavelength of 365 nm, with some intensity at 405 nm, 436 nm, and in the visible region. The total intensity of the UV radiation is about 20 mW/cm<sup>2</sup> with a 10-cm distance in air between the sample and the UV source. The intensity of solar radiation is about 136 mW/cm<sup>2</sup>, in which more than 70% of the intensity is concentrated in the near-UV, visible, and near-IR regions between 320 and 1000 nm (28).

**Photodecomposition.** In the main body of this study, the photoinduced decomposition of TCE irradiated with UV light was carried out in the following three modes: (1) open to air, (2) under the passage of air, and (3) under the passage of O<sub>2</sub>(g). For each of these three modes, a mixture of TCE and Ca-montmorillonite with a 1:1 weight ratio (e.g., 2.00 g of each) was placed in a quartz tube, which was connected to a water-cooled condenser to minimize evaporation of TCE during UV irradiation. The TCE was mixed with Ca-montmorillonite as well as possible by tapping and shaking the tube, left to stand in the dark for about an hour, and then irradiated with the UV lamp for various periods of time. A portion of the resulting mixture after irradiation was subjected to solid-state <sup>13</sup>C NMR analysis. The remaining portion of the solid was extracted with deuteriochloroform (e.g., 1.0 g of the UV irradiated mixture was stirred with 5.0 mL deuteriochloroform) at room temperature for ~12 h and filtered. The filtrate was subjected to liquid-solution <sup>13</sup>C NMR analysis. <sup>13</sup>C NMR results obtained on a TCE/Ca<sup>2+</sup>-montmorillonite sample that had been equilibrated for 24 h, prior to a 24-hour irradiation, are qualitatively very similar to, albeit quantitatively different than, an analogous sample equilibrated for 1 h.

**Detection of Gas Products.** To detect the production of suspected gas-phase products (CO<sub>2</sub>, HCl, and phosgene), either air or O<sub>2</sub>(g) was passed through the reaction vessel,

and the exit gas was analyzed. In the air case, before the air entered the quartz reaction vessel, it was bubbled through a trap containing a saturated aqueous Ba(OH)<sub>2</sub> solution to remove CO<sub>2</sub> in the air and then passed through a tower of sodium hydroxide pellets to remove any remaining CO<sub>2</sub> and to dry the air before being introduced via an adjustable flow valve into the reaction vessel. On the exit side of the quartz reactor tube, the gas (air or O<sub>2</sub>, plus volatile reaction products) was passed through a series of traps in the following sequence: (a) aqueous 1.0 M AgNO<sub>3</sub> solution (pH = 1) to detect HCl via AgCl(s) formation; (b) two successive traps with saturated aqueous Ba(OH)<sub>2</sub> solution to detect CO<sub>2</sub> via formation of BaCO<sub>3</sub>(s), and (c) a final trap containing silicone oil to minimize diffusion of atmospheric CO<sub>2</sub> back into the system. In a separate set of experiments, two successive traps with aqueous aniline solution (0.02 M) were used to detect phosgene via the formation of 1,3-diphenylurea.

**NMR Spectroscopy.** Solid-state <sup>13</sup>C NMR spectra were obtained at 25.27 MHz by the DP-MAS technique (direct polarization-magic angle spinning, i.e., no cross polarization) with high-power <sup>1</sup>H decoupling, on a home-built 100 MHz (<sup>1</sup>H frequency) spectrometer, using a Chemagnetics Phoenix data system, with a 90° pulse length of 6.5 μs and a recycle delay of 3 s. A Kel-F sample cell with an O-ring sealed cap was inserted into a Chemagnetics 14 mm PENCIL rotor and was used at a spinning speed of about 3 kHz. Liquid-solution <sup>1</sup>H and <sup>13</sup>C NMR spectra were obtained at 300.13 and 75.47 MHz, respectively, on a Bruker AC-300P spectrometer.

## Results and Discussion

The photochemical degradation of TCE on Ca-montmorillonite was initially examined under the following three sets of conditions: (1) The reaction mixture of TCE and Ca-montmorillonite in a quartz tube was evacuated at ~10<sup>-3</sup> Torr to remove oxygen and then sealed; the sealed sample was subjected to UV irradiation for 2 days. The solid-state <sup>13</sup>C NMR spectrum of the resulting sample (Figure 1A) shows only the signals of TCE at 116 and 123 ppm, for the CHCl and CCl<sub>2</sub> carbons, respectively. No decomposition of TCE was observed under these conditions. (2) The quartz tube containing the reaction mixture of TCE and Ca-montmorillonite was sealed without evacuation and then was subjected to UV irradiation. After 2 days of UV irradiation, the solid-state <sup>13</sup>C NMR spectrum, shown in Figure 1B, displays new signals with very small intensity, in addition to those of TCE; this indicates that photochemical degradation of TCE has occurred to a very small extent in this system. (3) The experiment was conducted with the system open to air, as described in the Experimental Section; the solid-state <sup>13</sup>C NMR spectrum of the reaction mixture after 2 days of UV irradiation (Figure 1C) shows large signals besides those of TCE. These results indicate that oxygen and/or water is necessary for the efficient photochemical degradation of TCE over Ca-montmorillonite.

Studies of intermediates and products in the photocatalytic degradation of TCE over TiO<sub>2</sub>(s) have previously been examined under various oxygen and water concentrations (11, 29, 30). All experiments corresponding to the formation of oxygen-containing intermediates and products, such as dichloroacetyl chloride, phosgene, CO<sub>2</sub>, and CO, have been performed at high oxygen concentration or in ambient air, in the presence or absence of water (11, 13, 14, 16, 20). In contrast, the formation of various chlorinated organic intermediates/products, e.g., pentachloroethane, hexachloroethane, tetrachloroethylene, CHCl<sub>3</sub>, and CCl<sub>4</sub>, which do not contain oxygen, were observed at relatively low oxygen concentrations (29, 30).

The decomposition of TCE on Ca-montmorillonite described in case (3) above (Figure 1C) is apparently due to photooxidation. In the absence of the UV irradiation, no

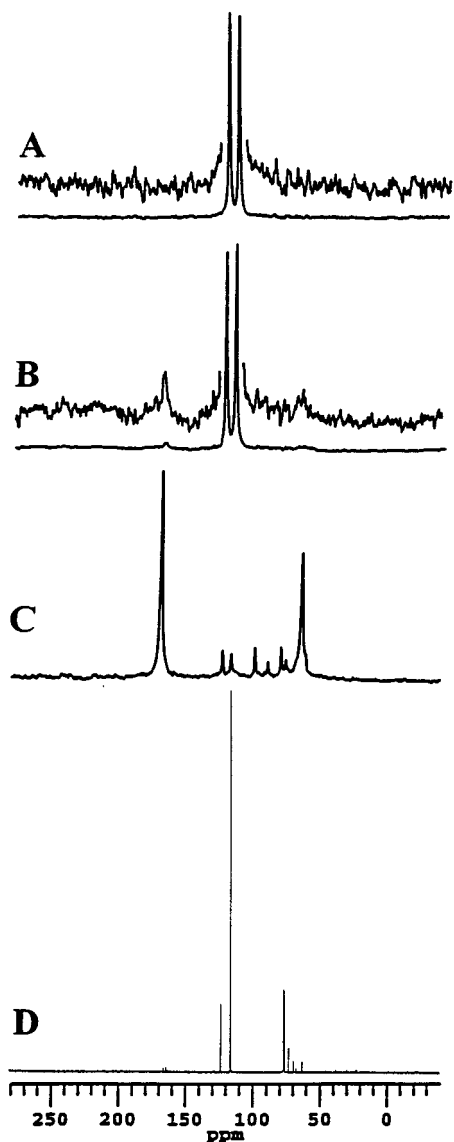


FIGURE 1. Solid-state  $^{13}\text{C}$  DP-MAS NMR spectra of TCE adsorbed on Ca-montmorillonite after 48-h UV irradiation with the system (A) evacuated at  $10^{-3}$  Torr and sealed; (B) sealed without evacuation; (C) open to air (each spectrum was obtained with a  $90^\circ$  pulse length of  $6.5 \mu\text{s}$ , a recycle delay of 3 s, and 10 000 scans.); and (D) liquid-sample  $^{13}\text{C}$  NMR spectrum of liquid TCE after UV irradiation for 48 h (1000 scans); the large intensity difference between the two  $\text{sp}^2$  peaks (116 and 123 ppm) is due to differences in spin lattice relaxation and NOE behaviors.

decomposition was detected for a sample of TCE adsorbed on Ca-montmorillonite over a period of weeks. Many studies have been reported on the gas phase and aqueous-solution oxidation of TCE in which control experiments showed no photooxidation of TCE under UV irradiation ( $\lambda > 290 \text{ nm}$ ) in the absence of a catalyst (11, 13, 16, 20). Nevertheless, a control experiment was carried out in this study in the absence of clay or any other solid adsorbent, i.e., the photodecomposition of pure liquid TCE under the conditions described in case (3) above. Surprisingly, about 10% of the TCE was decomposed, mainly converted to dichloroacetyl chloride, dichloroacetic acid and trichloroethylene oxide (trichlorooxirane), during a 48-h UV irradiation (Figure 1D); this can be compared to >95% for the  $\text{Ca}^{2+}$ -montmorillonite case (or >98% for the silica case). Since the wavelengths of the available intensity of the UV source in this study are above 360 nm, the photodecomposition of trichloroethylene

on Ca-montmorillonite cannot be due primarily to a direct, homogeneous photooxidation of TCE.

Figure 2 shows solid-state  $^{13}\text{C}$  NMR spectra of TCE/Ca-montmorillonite samples after UV irradiation for various periods of time with the system open to ambient air, as described in the Experimental Section. Figure 2A shows the  $^{13}\text{C}$  NMR spectrum of TCE/Ca-montmorillonite before UV irradiation; this spectrum displays only the two peaks at 116 and 123 ppm due to two  $\text{sp}^2$  carbons of TCE. After UV irradiation for 6 h, some small  $^{13}\text{C}$  signals, in addition to those of TCE, are seen (Figure 2B). With increasing irradiation time for 12, 24, and 48 h (Figure 2 (parts C–E)), the intensities of these signals increase, as the intensities of TCE peaks decrease. The major signals of the photooxidation products at 65 and 168 ppm are assigned to dichloroacetic acid; the signals with relatively small intensities at 80 and 100 ppm are assigned to pentachloroethane. These assignments were confirmed by liquid-solution  $^{13}\text{C}$  NMR spectra of chloroform-*d* extracts. Upon continued irradiation to 3 days (72 h), the TCE signals at 116 ppm and 123 ppm disappeared (Figure 2F); liquid-solution  $^{13}\text{C}$  NMR of the chloroform-*d* extract of the 72-h irradiated sample and an authentic sample confirmed that the shoulder at 166 ppm and the signal at 90 ppm in spectrum of Figure 2F are due to trichloroacetic acid. The intensity-vs-time patterns in Figure 2 suggest that formation of trichloroacetic acid may result from the photooxidation of pentachloroethane. The  $\text{TiO}_2(\text{s})$  catalyzed photooxidation of pentachloroethane to trichloroacetic acid under UV irradiation has been reported previously by Nimlos et al (13, 20). Table 1 summarizes the product distribution of the TCE photodegradation on different catalysts or adsorbents.

Further irradiation of the TCE/Ca-montmorillonite system results in the decomposition of dichloroacetic acid and other products into volatile species (e.g.,  $\text{CO}_2$ , HCl, phosgene, etc.), which escape from the system. Solid-state  $^{13}\text{C}$  DP-MAS spectra of the samples prepared with irradiation times of 5, 10, and 20 days (Figures 2G, 2H, and 2I) show that the total NMR-detectable  $^{13}\text{C}$  signals are dramatically decreased during the prolonged UV irradiation periods. In addition to loss of signal intensity, an apparent peak broadening can be seen in the spectra corresponding to the samples irradiated for 10 and 20 days (Figure 2 (parts H and I)). The observed line broadening might result from reactions of dichloroacetic acid and trichloroacetic acid with surface hydroxyl groups to form surface-bound species, with a variety of local structures; the resulting surface-based  $^{13}\text{C}$  chemical shift dispersion could provide a source of inhomogeneous broadening. The suggestion that the broad peaks in Figure 2 (parts H and I) are due to surface-bound species is supported by the fact that, when the sample of Figure 2H was extracted with deuteriochloroform (which should remove physisorbed or nonadsorbed species), the broad peaks remained in the  $^{13}\text{C}$  NMR spectrum (not shown here) of the extraction residue. The formation of ester linkages between the intermediates and the surface has been reported previously for the  $\text{TiO}_2(\text{s})$  photodegradation system (21, 22).

The Ca-montmorillonite catalyzed photodecomposition of TCE in this study occurs over a period of days; in contrast, the  $\text{TiO}_2(\text{s})$  catalyzed photodegradation of TCE under similar conditions is complete in a period of hours. Dichloroacetyl chloride, trichloroacetyl chloride, dichloroacetylaldehyde and trichloroacetaldehyde have been observed previously as intermediate products in the  $\text{TiO}_2(\text{s})$ -catalyzed photooxidation of TCE (11–17, 21, 22). None of these products were detected in the solid-sample  $^{13}\text{C}$  NMR experiments of this study. The absence of dichloroacetyl chloride could possibly be due to its hydrolysis to dichloroacetic acid under the influence of moisture in the clay and in air; dichloroacetic acid is a major photooxidation intermediate/product found

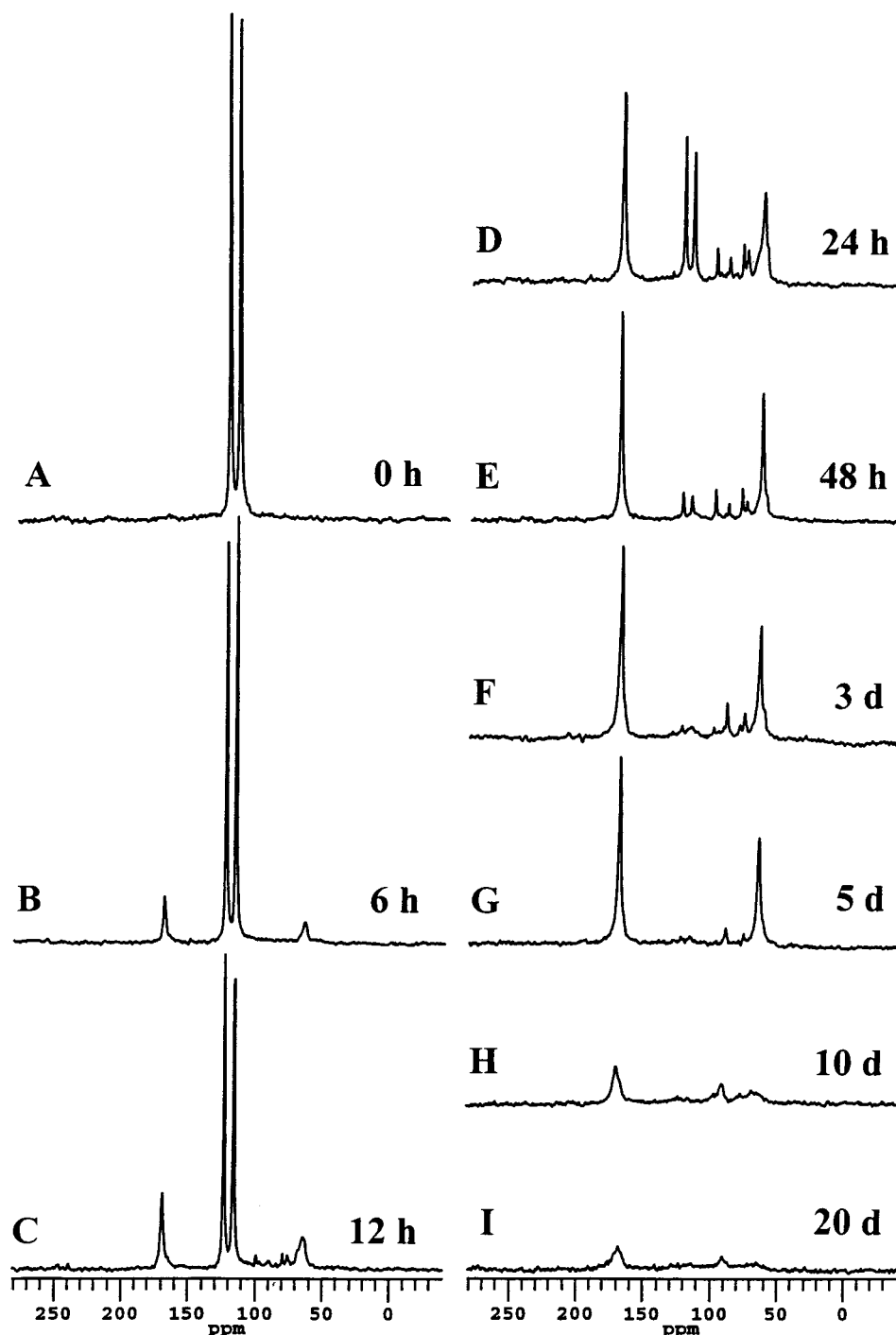


FIGURE 2. Solid-state  $^{13}\text{C}$  DP-MAS NMR spectra of TCE adsorbed on Ca-montmorillonite after UV irradiation for various periods of time, as indicated. Each spectrum was obtained with a  $90^\circ$  pulse length of  $6.5 \mu\text{s}$ , a recycle delay of 3 s, and 10 000 scans.

in this study, while Raftery and co-workers found that, in the photooxidation of TCE in the presence of  $\text{O}_2$  and powdered  $\text{TiO}_2$  catalyst in a sealed tube, dichloroacetyl chloride was a major long-lived intermediate (21, 22).

It is not clear on the basis of the present results what the precise role of Ca-montmorillonite is in the photoinduced conversions. Clay minerals are major soil components that typically have large surface areas, strong adsorbing properties, and important catalytic characteristics. The basic structure of Ca-montmorillonite is composed of parallel stacked sheets, each being a composite of two tetrahedral layers and one octahedral layer, with an interlayer space in which water and hydrated metal ions (e.g.,  $\text{Ca}^{2+}$ ) are situated (31).

Due to their layered silicate structure and cation-exchanged properties, clays can have oxidizing centers, e.g.,  $\text{Fe}^{3+}$  ions or silyloxy radicals ( $\text{O}_3\text{SiO}^\bullet$ ) on their surface and in the interlayers (32). Such species conceivably can initiate free radical processes. It has been reported that a single electron-transfer mechanism is operative for the oxidative dechlorination and dimerization of 4-chloroanisole on clays (33). The presence of radical intermediates in the clay-organic complex was confirmed by ESR and IR spectroscopy. Furthermore, the observation of the photooxidation product, pentachloroethane, in this study suggests that a mechanism involving chlorine atoms might be operative in the system on which we are reporting here. According to this kind of

TABLE 1. Product Distribution in the Photoassisted Decomposition of TCE under Various Conditions

system studied	detection method	major products	ref
TCE/TiO <sub>2</sub> (in oxygen)	NMR	carbon dioxide, carbon monoxide, dichloroacetyl chloride, dichloroacetic acid, pentachloroethane, phosgene, trichloroacetic acid	(21), (22)
TCE/TiO <sub>2</sub> (in oxygen)	IR	carbon dioxide, carbon monoxide, dichloroacetyl chloride, phosgene, hydrochloric acid	(11), (20)
TCE/TiO <sub>2</sub> (low oxygen concn)	MS	carbon tetrachloride, chloroform, hexachloroethane, pentachloroethane, tetrachloroethylene	(29)
TCE/TiO <sub>2</sub> (in water)	GC/MS	dichloroacetaldehyde, dichloroacetic acid, trichloroacetaldehyde, trichloroacetic acid	(34)
TCE/Clay, TCE/Soil (ambient air)	NMR	carbon dioxide, dichloroacetic acid, pentachloroethane, phosgene, trichloroacetic acid	this study

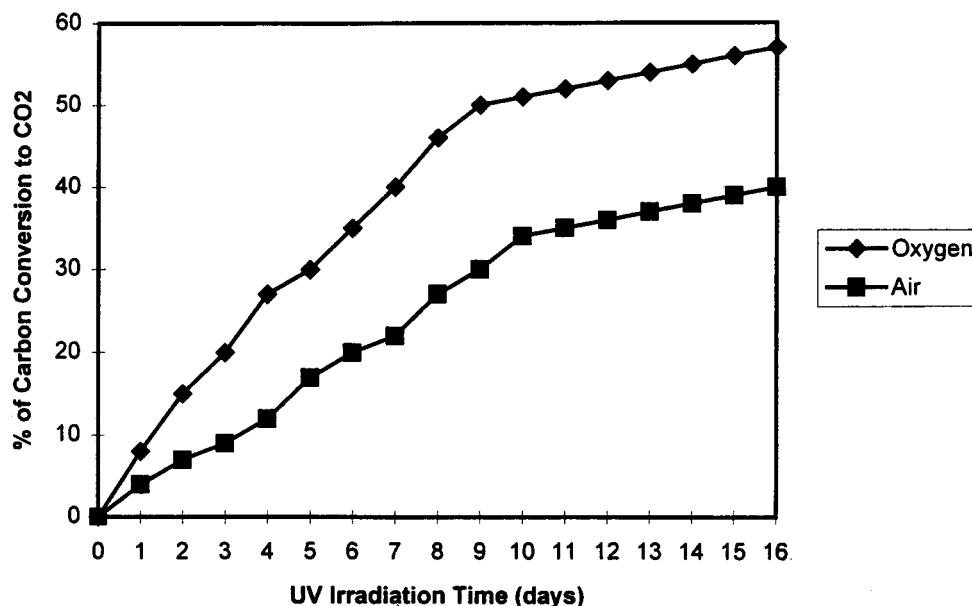
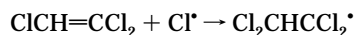
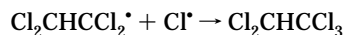


FIGURE 3. Conversion of the carbon content of TCE to CO<sub>2</sub>, monitored as a function of UV irradiation time.

hypothesis (13, 30), a Cl atom adds to the carbon atom bonded to hydrogen.



The resulting alkyl radical would combine with another Cl atom or abstract a chlorine atom from another source to produce pentachloroethane.



The gas-phase products produced from the photooxidation of TCE over Ca-montmorillonite were detected through analysis of the contents of a series of traps containing (1) aqueous aniline solution, (2) 1.0 M AgNO<sub>3</sub>(aq), and (3) Ba(OH)<sub>2</sub>(aq), as described in the Experimental Section. In both cases, with air or oxygen used as a carrier gas, detection of 1,3-diphenylurea in the aniline trap by liquid-sample <sup>13</sup>C NMR indicates the production of phosgene from the photooxidation reaction (34). Small quantities of phosgene were detected in this study; i.e., 0.22 mmol of phosgene was formed (from 15 mmol TCE) when O<sub>2</sub>(g) was used as a carrier gas over a 20-day period, while 0.18 mmol of phosgene was detected when air was used as a carrier gas over a 20-day period. The low yield of phosgene in this study could result from the reaction of phosgene with ambient moisture (H<sub>2</sub>O) to yield CO<sub>2</sub> and HCl. Raftery and co-workers have reported that adsorbed water in the TiO<sub>2</sub> catalyst was found to greatly reduce the formation of phosgene (22).

An aqueous AgNO<sub>3</sub> solution was used to trap HCl formed from the decomposition of TCE; in both cases, when either air or O<sub>2</sub>(g) was used as the carrier gas, very small amounts of AgCl(s) were found. Perhaps much of the HCl produced from the photooxidation is absorbed on/in the Ca-montmorillonite and is not released. This view is supported by the fact that, when the solid sample resulting from photo-decomposition was washed with water, a large amount of AgCl(s) was formed when AgNO<sub>3</sub>(aq) was added to the aqueous wash. In contrast, an aqueous wash of the original (UV-irradiated) clay yielded only a minor cloudiness, no precipitate, when treated with AgNO<sub>3</sub>(aq).

When either air or oxygen was used as the carrier gas, large amounts of white precipitate were observed in the first Ba(OH)<sub>2</sub>(aq) trap that follows the AgNO<sub>3</sub>(aq) trap in the decomposition of TCE. The trapping efficiency of CO<sub>2</sub> by Ba(OH)<sub>2</sub>(aq) in the first such trap was confirmed by the fact that little precipitate was observed in the second Ba(OH)<sub>2</sub>(aq) trap.

Figure 3 shows plots of the percentage of the total carbon of TCE converted to carbon dioxide vs irradiation time. In the case in which a flow of air was employed, it was determined that the TCE-to-CO<sub>2</sub> conversion over a 16-day period was ~40%. In the case in which a flow of O<sub>2</sub>(g) was employed, ~57% of the TCE was converted to CO<sub>2</sub> over a 16-day period. By comparison, in the photooxidation of the TCE reported by Raftery and co-workers (22), the yield of CO<sub>2</sub> was calculated to be 50–60% of the initial TCE

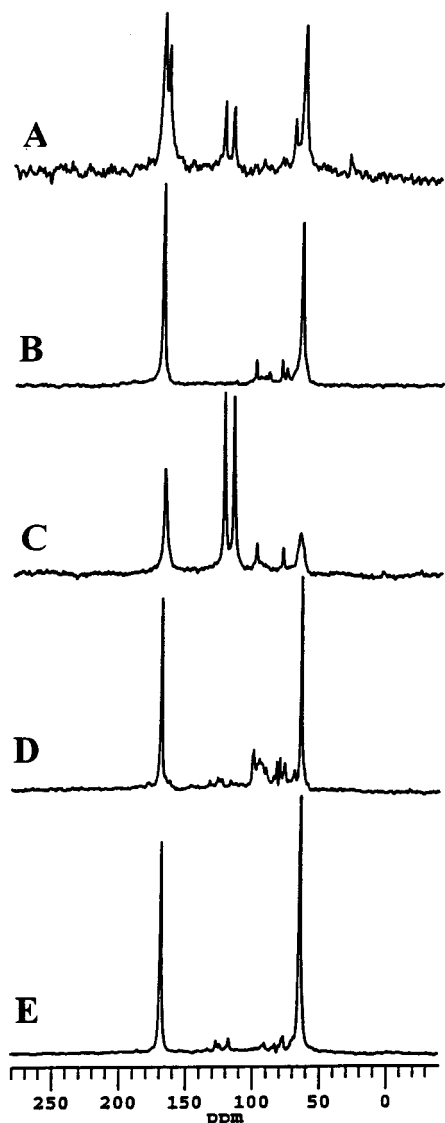


FIGURE 4. Solid-state  $^{13}\text{C}$  DP-MAS NMR spectra of TCE on (A) whole soil; (B)  $\text{Zn}^{2+}$ -exchanged montmorillonite; (C)  $\text{Cu}^{2+}$ -exchanged montmorillonite; (D) kaolinite; and (E) silica gel, after UV irradiation for 48 h. Each spectrum was obtained with a  $90^\circ$  pulse length of  $6.5 \mu\text{s}$ , a recycle delay of 3 s, and 10 000 scans.

concentration over a 4-h period, when  $\text{TiO}_2$  was used as a catalyst.

The photoinduced decomposition of TCE on a whole soil yields a set of degradation products that is similar to those produced in the photoinduced decomposition of TCE on Ca-montmorillonite. The  $^{13}\text{C}$  DP-MAS spectrum shown in Figure 4A was obtained from the mixture of TCE and whole soil after 48 h of UV irradiation with the system open to ambient air. In addition to spectral features due to some unreacted TCE (peaks at 117 and 124 ppm), the major peaks at 65 and 170 ppm in Figure 4A are due to the formation of dichloroacetic acid. One can see two shoulders at 72 and 166 ppm, which might correspond to the formation of chemical linkages between dichloroacetic acid and humic materials.

To estimate the efficiency of other solid substrates on the photodecomposition of TCE,  $\text{Zn}^{2+}$ -exchanged and  $\text{Cu}^{2+}$ -exchanged Ca-montmorillonites were also examined. Figure 4 (parts B and C) shows the solid-state  $^{13}\text{C}$  DP-MAS spectra of samples of TCE adsorbed on  $\text{Zn}^{2+}$ -exchanged and  $\text{Cu}^{2+}$ -exchanged montmorillonites after 48 h of UV irradiation with

the systems open to air. The spectrum of the sample based on  $\text{Zn}^{2+}$ -exchanged montmorillonite (Figure 4B) displays features that are very similar to those of the corresponding Ca-montmorillonite sample (Figure 2E); the TCE peaks at 116 and 123 ppm are gone, and the major products are dichloroacetic acid at 65 and 169 ppm and pentachloroethane at 80 and 100 ppm. However, in the spectrum of the sample based on  $\text{Cu}^{2+}$ -exchanged montmorillonite (Figure 4C), large TCE peaks are still present, which implies that  $\text{Cu}^{2+}$  is not as efficient as either  $\text{Zn}^{2+}$  or  $\text{Ca}^{2+}$  in promoting the photooxidation of TCE on montmorillonite under these experimental conditions. It is not clear if decreased efficiency of the photooxidation is due explicitly to the properties of  $\text{Cu}^{2+}$  sites or due to the change of adsorption properties of the  $\text{Cu}^{2+}$ -exchanged clay from those of the original Ca-montmorillonite.

Photodecomposition of TCE adsorbed on kaolinite (as received) and on silica gel (10 wt % water added) were also examined with the systems open to air and 48 h of UV irradiation. The solid-state  $^{13}\text{C}$  DP-MAS NMR spectra of the TCE/kaolinite mixture and TCE/silica gel mixture after 48 h of UV irradiation are shown in Figure 4 (parts D and E). In both cases, TCE was decomposed, and dichloroacetic acid was found to be the major product.

While the time scale is roughly an order of magnitude longer in the studies reported here than for the photoinduced decomposition of trichloroethylene on  $\text{TiO}_2(\text{s})$ , what appear to be similar photodecomposition processes seem to occur on soil and soil components. Thus, these results provide qualitatively useful information on the likely chemical behavior of TCE at the air-soil interface. As far as environmental quality is concerned, dichloroacetic acid is a known animal carcinogen, and its potency is greater than that of TCE (35, 36). Furthermore,  $^{13}\text{C}$  NMR is seen to be well suited to elucidating interesting and important chemical details of these processes.

#### Acknowledgments

This work was supported in part by AFOSR Grant F49620-95-0192 and DOE Grant DE-FG03-95ER14558. We would like to thank Dr. I-S. Chuang, Dr. H. Lock, Dr. J. Xiong, Mr. D. Keeler, Mr. R. Persik, and Mr. M. Seger for useful discussions and technical assistance.

#### Literature Cited

- (1) Maull, E. A.; Cogliano, V. J.; Scott, C. S.; Barton, H. A.; Fisher, J. W.; Greenberg, M.; Rhomberg, L.; Sorgen, S. P. *Drug Chem. Toxicol.* **1997**, *20*, 427.
- (2) Lewis, G. R. *1001 Chemicals in Everyday Products*; Van Nostrand Reinhold: New York, 1994; p 253.
- (3) *1996/97 Directory of Superfund Sites*; Environmental Data Associates, Inc. Eds.; Washington, D.C., 1996.
- (4) Gist, G. L.; Burg, J. R. *Toxicol. Indust. Health* **1995**, *11*, 253.
- (5) Bruckner, J. V.; Davis, B. D.; Blancato, J. N. *Crit. Rev. Toxicol.* **1989**, *20*, 31.
- (6) McCarty, P. L.; Goltz, M. N.; Hopkins, G. D.; Dolan, M. E.; Allan, J. P.; Kawakami, B. T.; Carrothers, T. J. *Environ. Sci. Technol.* **1998**, *32*, 88.
- (7) Sutfin, J. A.; Ramey, D. *Environ. Prog.* **1997**, *16*, 287.
- (8) Linsebigler, A. L.; Liu, G.; Yates, J. T., Jr. *Chem. Rev.* **1995**, *95*, 735.
- (9) Hoffmann, M. R.; Martin, S. T.; Choi, W.; Bahnemann, D. W. *Chem. Rev.* **1995**, *95*, 69.
- (10) Fox, M. A.; Dulay, M. T. *Chem. Rev.* **1993**, *93*, 341.
- (11) Fan, J.; Yates, J. T., Jr. *J. Am. Chem. Soc.* **1996**, *118*, 4686.
- (12) Phillips, L. A.; Raupp, G. B. *J. Mol. Catal.* **1992**, *77*, 297.
- (13) Nimlos, M. R.; Jacoby, W. A.; Blake, D. M.; Milne, T. A. *Environ. Sci. Technol.* **1993**, *27*, 732.
- (14) Jacoby, W. A.; Nimlos, M. R.; Blake, D. M. *Environ. Sci. Technol.* **1994**, *28*, 1661.
- (15) Yamazaki-Nishida, S.; Cervera-March, S.; Nagano, K. J.; Andeson, M. A.; Hori, K. *J. Phys. Chem.* **1995**, *99*, 15814.

- (16) Holden, W.; Marcellino, A.; Valic, D.; Weedon, A. C. *Photocatalytic Purification and Treatment of Water and Air*, Ollis, D. F.; Al-Ekabi, H. Eds.; Elsevier Science Publisher: Amsterdam, 1993; p 393.
- (17) Luo, Y.; Ollis, D. F. *J. Catal.* **1996**, *163*, 1.
- (18) Ahmed, S.; Ollis, D. F. *Solar Energy* **1984**, *32*, 597.
- (19) Pruden, A. L.; Ollis, D. F. *J. Catal.* **1983**, *82*, 404.
- (20) Nimlos, M. R.; Jacoby, W. A.; Blake, D. M.; Milne, T. A. *In Photocatalytic Purification and Treatment of Water and Air*, Ollis, D. F.; Al-Ekabi, H. Eds.; Elsevier Science Publisher: New York, 1993; p 387.
- (21) Hwang, S.-J.; Petucci, C.; Raftery, D. *J. Am. Chem. Soc.* **1997**, *119*, 7877.
- (22) Hwang, S.-J.; Petucci, C.; Raftery, D. *J. Am. Chem. Soc.* **1998**, *120*, 4388.
- (23) Maciel, G. E. *Science* **1984**, *226*, 282.
- (24) Tao, T.; Maciel, G. E. *Environ. Sci. Technol.* **1998**, *32*, 350.
- (25) Jurkiewicz, A.; Maciel, G. E. *Sci. Total Environ.* **1995**, *164*, 195.
- (26) Hinedi, Z. R.; Johnson, C. T.; Erickson, C. *Clays Clay Miner.* **1993**, *41*, 87.
- (27) Keeler, C.; Maciel, G. E. To be published.
- (28) *Encyclopedia of Applied Physics*, Trigg, G. L., Eds.; VCH: Verlagsgesellschaft, Weinheim, 1993; Vol. 18, p 397.
- (29) Hung, C.-H.; Mariñas, B. J. *Environ. Sci. Technol.* **1997**, *31*, 1440.
- (30) Hung, C.-H.; Mariñas, B. J. *Environ. Sci. Technol.* **1997**, *31*, 562.
- (31) Brindley, G. W.; Brown, G., Eds. *Crystal Structures of Clay Minerals and Their X-ray Identification*; Mineralogical Society Monograph 5; Spottiswoode Ballantyne Ltd.: London, 1984.
- (32) Balogh, M.; Laszlo, P. *Organic Chemistry Using Clays*, Springer-Verlag: New York, 1993; p 96.
- (33) Govindaraj, N.; Mortland, M. M.; Boyd, S. A. *Environ. Sci. Technol.* **1987**, *21*, 1119.
- (34) Crummett, W. B.; McLean, J. D. *Anal. Chem.* **1965**, *37*, 424.
- (35) Glaze, W. H.; Kenneke, J. F.; Ferry, J. L. *Environ. Sci. Technol.* **1993**, *27*, 177.
- (36) Bull, R. J.; Sanchez, I. M.; Nelson, M. A.; Larson, J. L.; Lansing, A. J. *Toxicology* **1990**, *63*, 341.

*Received for review April 29, 1998. Revised manuscript received September 8, 1998. Accepted September 21, 1998.*

ES980435A